Journal of the European Ceramic Society **11** (1993) 347–352

SEM and TEM/EDX Analysis of Model Interfaces in Multicomponent Electroceramics

N. Nicoloso, M. Haberkern

Max-Planck-Institut für Metallforschung, Institut für Werkstoffwissenschaft, Pulvermetallurgisches Laboratorium, Heisenbergstraße 5, D-7000 Stuttgart 80, Germany

A. LeCorre-Frisch

Thomson-LCC, Avenue du Colonel Prat, 21850 Saint Appollinaire, France

J. Maier

Max-Planck-Institut für Festkörperforschung, Heisenbergstraße 1, D-7000 Stuttgart 80, Germany

&

R. J. Brook

University of Oxford, Department of Materials, Parks Road, Oxford OX1 3PH, UK

(Received 6 July 1992; revised version received 3 August 1992; accepted 1 September 1992)

Abstract

The interfaces between $(Ni,Zn)Fe_2O_4$ and $MgTiO_3$ as well as between $MgTiO_3$ and RuO_2 glass—models for the interfaces in multicomponent electroceramics—have been investigated by SEM and combined TEM/EDX analysis. Under the preparation conditions involved (1400 K, 2 h), the local properties of both interfaces are mainly thermodynamically controlled. In the case of the ferrite–titanate system, a $<3\,\mu m$ thick interface is formed, consisting of a compositionally modified, cation-exchanged spinel phase, $Mg_{1+x}Fe_{2-2x}Ti_xO_4$, with $x = 0{\cdot}66$, and a pseudobrookite phase, $Mg_xFe_{2-2x}Ti_{1+x}O_5$, with $x = 0{\cdot}75$. Concerning the interface properties of $MgTiO_3$–RuO_2 glass, interdiffusion of Ti and Mg appears to be the dominant process below 1100 K, whereas at higher temperature several new phases can be clearly identified in the $<10\,\mu m$ thick interface region, e.g. $MgSiO_3$ and $PbTiO_3$.

$(Ni,Zn)Fe_2O_4$–$MgTiO_3$ bzw. RuO_2-Glas–$MgTiO_3$-Grenzflächen—prototypisch für keramische integrierte Bausteine—wurden durch Ko-Sintern (1400 K, 2 h) hergestellt und mit Hilfe von SEM- und TEM/EDX-Aufnahmen analysiert. Unter den angegebenen Bedingungen stellen sich in beiden Systemen Grenzschichten ein, deren lokale Eigenschaften vorwiegend thermodynamisch kontrolliert sind. Im Falle des Ferrit–Titanatsystems bildet sich eine $<3\,\mu m$ dicke Grenzschicht aus einer kationenausgetauschten Spinellphase, $Mg_{1+x}Fe_{2-2x}Ti_xO_4$, mit $x = 0{\cdot}66$, und einer Pseudobrookitphase, $Mg_xFe_{2-2x}Ti_{1+x}O_5$, mit $x = 0{\cdot}75$. Im System RuO_2-Glas–$MgTiO_3$ überwiegt bei Temperaturen <1100 K die Interdiffusion von Ti und Mg. Bei höheren Temperaturen entstehen neue Phasen. In der $<10\,\mu m$ dicken Grenzschicht lassen sich insbesondere $MgSiO_3$ und $PbTiO_3$ nachweisen.

Les auteurs ont examiné, par MEB et MET combinées à une analyse EDX, les interfaces entre $(Ni,Zn)Fe_2O_4$ et $MgTiO_3$ et entre $MgTiO_3$ et RuO_2 vitreux. Ces systèmes constituent des modèles de céramiques multicomposants. Dans les conditions de préparation (1400 K, 2 h), les propriétés locales des deux interfaces sont proches de l'équilibre thermodynamique. Dans le cas du système ferrite–titanate, une interface d'épaisseur $<3\,\mu m$ est formée. Elle consiste en une phase de spinelle modifiée par substitution de cations ($Mg_{1+x}Fe_{2-2x}Ti_xO_4$ avec $x = 0{\cdot}66$) et en phase pseudobrookite ($Mg_xFe_{2-2x}Ti_{1+x}O_5$ avec $x = 0{\cdot}75$). En ce qui concerne l'interface entre $MgTiO_3$ et le RuO_2 vitreux, l'interdiffusion de Ti et Mg semble le processus dominant sous 1100 K, tandis qu'à plus haute température, plusieurs nouvelles phases peuvent être clairement identifiées dans une

Journal of the European Ceramic Society 0955-2219/93/$6.00

région d'interface d'épaisseur <10 μm, entre-autres $MgSiO_3$ et $PbTiO_3$.

1 Introduction

Today's functional ceramics serve almost exclusively as passive components in electronic circuits. Although these single-function electronic components have been miniaturized to sizes compatible with current surface-mounting technologies, they remain the bulky part of electronic systems. For higher integration, the next innovative step will be the production of multicomponent systems, i.e. passive ceramic chips combining several single functions—see Ref. 1 for detailed information. Typical applications of these electroceramic circuits are high- or low-frequency filters or passive electronic circuits in a corrosive atmosphere at elevated temperature, e.g. electronics for the lambda probe in cars.

The present study is concerned with some of the critical aspects of this technique: powder processing, confirmation of the compatibility between materials and determination of the interface structure. In particular, the starting materials have to be appropriately tailored to establish the desired microstructure and to minimize the chemical reactivity. Co-sintering of the different materials proves to be the critical preparation step, since even at the comparatively low sintering temperature of 1200 K appreciable interdiffusion and chemical reaction occurs. Hence, each of the interfaces, ferrite–titanate and titanate–RuO_2 glass, may alter the bulk properties as soon as the size of the electroceramic approaches the dimensions of the interface. Keeping in mind that the individual components, resistors R, capacities C and inductance L, have required tolerances <5%, both the reproducibility for the co-sintering process and the ratio of bulk to interface properties will be of crucial importance for micro-sized ceramic circuits.

Therefore the authors have started a series of investigations on typical RC and LC components consisting of a resistive or inductive layer (RuO_2 glass composite or Ni,Zn ferrite) on top of a dielectric layer ($MgTiO_3$). The TEM and EDX studies yield information about the microstructure, composition and spatial extension of the respective interfaces $MgTiO_3$–RuO_2 glass and $MgTiO_3$–ferrite, and allow an estimate of the minimum component size compatible with this method to be made.

Initial studies of the electrical properties of these monolithic ceramic circuits and, in particular, of RuO_2 glass composites have revealed contributions from different transport mechanisms.[1] A detailed description of the various transport properties (hopping between RuO_2 clusters, tunnelling between nanosized RuO_2 particles within large clusters, etc.) is given in Ref. 2.

2 Experimental

RuO_2 glass composites with resistivities ranging from 1 to $10^6\,\Omega$cm have been prepared by mixing RuO_2 powder (grain size = 20 nm) with borosilicate glass (grain size = 1·5 μm) in ethanol for 1 h. After drying and sieving, an organic binder was added to obtain a resistive ink. This paste was screen-printed onto tape-cast $MgTiO_3$ and co-sintered at 1100 and 1200 K for 0·5 or 1 h, respectively, to obtain electroceramic RC components. Similarly, LC components were prepared by lamination and co-sintering at 1400 K for 2 h on tape-cast $MgTiO_3$ and $(Ni,Zn)Fe_2O_4$.

After cutting these sandwich-type specimens perpendicular to the RC or LC interfaces, the usual preparation steps for TEM studies were carried out. In the final step, the thickness of the sample was reduced by ion beam thinning until a small hole appeared in the centre of the sample. At some locations the hole is right at the interface; the thickness at the edge of the hole does not exceed 100 nm. Difficulties with the ion beam thinning process arise from the different thinning rates of the materials: the ferrite is much more readily thinned than the titanate and the RuO_2 glass composite. The present TEM investigations were performed with a JEOL 2000 EX transmission electron microscope equipped with an energy dispersive X-ray analyser. Especially in the case of light elements like Mg, the k-factor[3,4] has to be precisely known for quantitative EDX analysis. Therefore the analyser was calibrated using several standard materials (Mg_2Si, $TiSi_2$, etc.).

3 Results and Discussion

3.1 $MgTiO_3$–RuO_2 glass interface

Figure 1 shows a typical SEM overview of a (Si-enriched) $MgTiO_3$–RuO_2 glass interface prepared at 1200 K. The SEM and EDX analysis (Fig. 2) reveal an interface which is less than 10 μm thick and mainly consisting of $MgSiO_3$ and $PbTiO_3$. Note that $PbTiO_3$ and $MgSiO_3$ are predominantly formed at those interface parts which are in intimate contact with the titanate or the RuO_2 glass, respectively. As expected, the thickness of the interface is decreased to <3 μm when the sintering temperature is lowered to 1100 K—see Fig. 3. The solubility of Ru in the interface is surprisingly low. Neither the formation of ruthenates nor appreciable dissolution of Ru (<1%) in borate glass was observed.

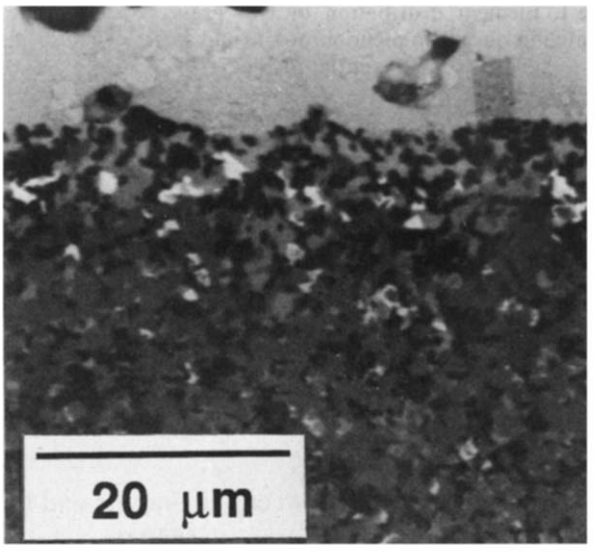

Fig. 1. SEM micrograph of the $MgTiO_3$–RuO_2 glass interface. White: RuO_2 glass; black: $MgTiO_3$. The spatial extension of the interface (<10 μm) is indicated by the two horizontal lines. For the preparation conditions see text.

3.2 MgTiO–ferrite interface

Figure 4 depicts the microstructure at high resolution of the $MgTiO_3$–ferrite interface. EDX analysis for the elements Fe, Mg, Ni, Ti and Zn was carried out within distances ±500 nm from the centre of the interface (dark spots).

As shown in Fig. 5(a), the Fe concentration ranges from about 23 to 16 at.%, whereas the Ti concentration changes drastically within a few nanometres from about 22 to 60 at.%. The Mg concentration stays constant at about 24 at.% in the ferrite and

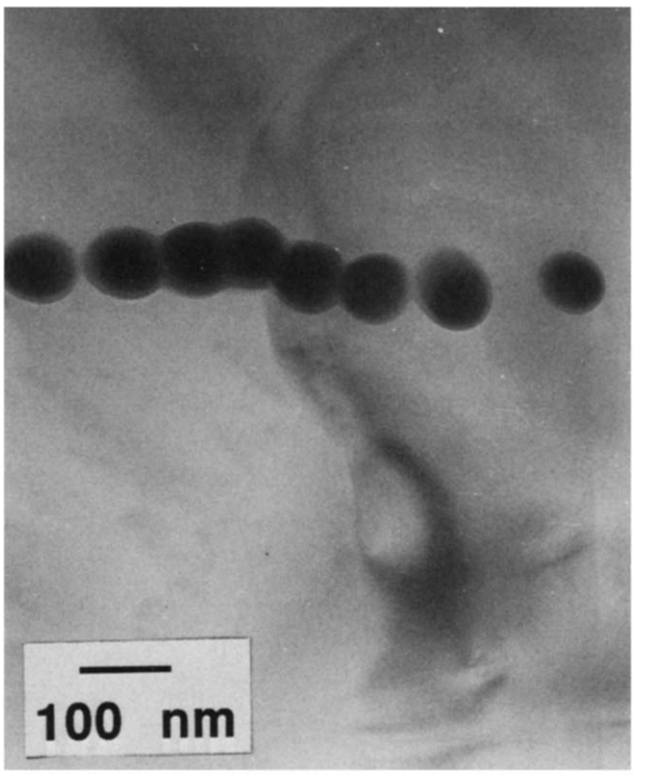

Fig. 4. TEM overview of the $MgTiO_3$–$(Ni,Zn)Fe_2O_4$ interface. EDX analysis has been performed at the dark spots.

titanate phase (Fig. 5(b)). The elements Ni and Zn interdiffuse only weakly. In comparison to Ni, however, Zn is strongly enriched in the ferrite part of the interface (6 at.% Ni and 26 at.% Zn to be compared with bulk ferrite concentrations of 13·5 at.% Ni and 12 at.% Zn, respectively).

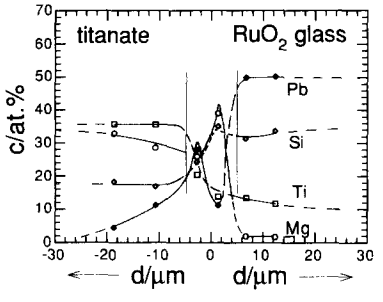

Fig. 2. EDX analysis of $MgTiO_3$–RuO_2 glass interface prepared at 1200 K for 1 h. The spatial extension of the interface (<10 μm) is indicated by the two vertical lines.

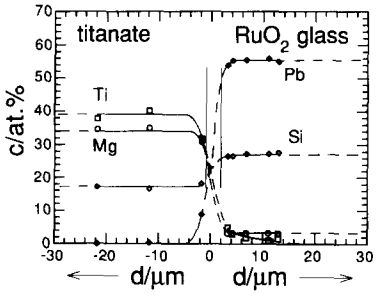

Fig. 3. EDX analysis of $MgTiO_3$–RuO_2 glass interface prepared at 1100 K; 0·5 h. Note that there is no clear indication of $MgSiO_3$ and $PbTiO_3$ phase formation as in Fig. 2.

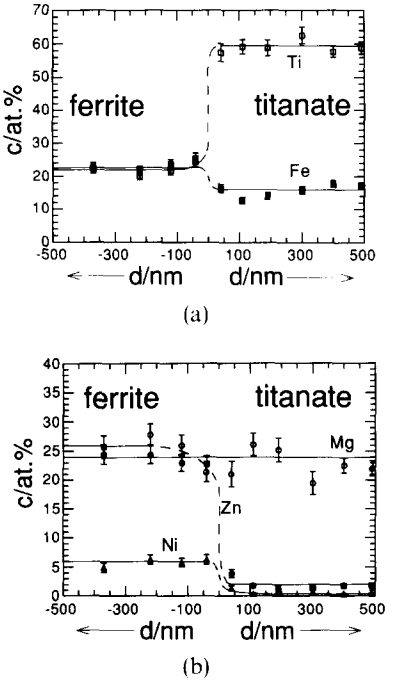

Fig. 5. EDX analysis of the $MgTiO_3$–$(Ni,Zn)Fe_2O_4$ interface co-sintered at 1400 K for 2 h. Range: ±500 nm. The typical error of the element distribution is represented by the corresponding error bars.

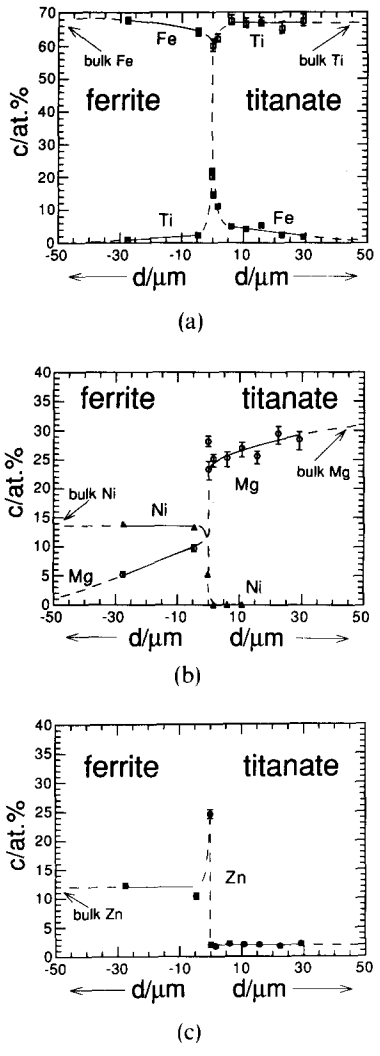

Fig. 6. EDX analysis of the $MgTiO_3$–$(Ni,Zn)Fe_2O_4$ interface co-sintered at 1400 K for 2 h. Range: $\pm 50\,\mu m$. The typical error is represented by the corresponding error bars.

To follow the interdiffusion across the whole interface, the EDX analysis was extended to distances $0 \leq d \leq \pm 30\,\mu m$. The dashed lines in Fig. 6(a)–(c) indicate the bulk values of the different elements in the ferrite and titanate parts of the interface. At distances greater than approximately $\pm 30\,\mu m$ the normal bulk concentrations for the ferrite and titanate constituents are found; exceptions occur only for $MgTiO_3$. Since standard grade $MgTiO_3$ always contains excess TiO_2, grains with the compositions $MgO.TiO_2$ and $MgO.2TiO_2$ are inhomogeneously distributed in the titanate part of the interface. Close to the interface nearly all the grains consist of $MgTi_2O_5$.

As shown in Fig. 6(a) and (b), the interdiffusion of Fe, Mg and Ti is remarkably high, since even at distances $d > \pm 30\,\mu m$ these elements can be detected in amounts of more than 1 at.% in the respective interface part. In the titanate part of the interface, Fe is more strongly enriched than Ni and Zn. Note that the Zn value is constant in the titanate part, due to the admixture of Zn (2 at.%) to minimize the

Table 1. Element distribution of two grains at the ferrite–titanate interface with pseudobrookite and spinel structure (see P1 and P2 in Fig. 7)

	Metal	c_m (*at.%*)	
$Mg_xFe_{2-2x}Ti_{1+x}O_5$, pseudobrookite, $x_1 \approx 0.75$	Fe	16·0	P1
	Mg	24·0	
	Ti	60·0	
$Mg_{1+x}Fe_{2-2x}Ti_xO_4$, spinel, $x_2 \approx 0.66$	Fe	22·0	P2
	Mg	24·0	
	Ni	6·0	
	Zn	26·0	
	Ti	22·0	

difference in expansion between the titanate and the ferrite (Fig. 6(c)).

The observation that only $MgTi_2O_5$ and no $MgTiO_3$ can be detected close to the ferrite–titanate interface provides a clue to the understanding of the interface properties. It suggests that the interface region mainly consists of two modifications of the starting materials $(Ni,Zn)Fe_2O_4$ and $MgTiO_3$. According to the MgO–TiO_2–Fe_2O_3 phase diagram (Fig. 7), $Fe_2O_3.TiO_2$ and $MgO.2TiO_2$—but not $MgO.TiO_2$—exist in equilibrium with $MgO.Fe_2O_3$ and $2MgO.TiO_2$. Fe from the ferrite phase dissolves in $MgO.TiO_2$ up to its equilibrium activity value, where the Fe-rich $MgO.TiO_2$ phase coexists with two other phases: a spinel and a pseudobrookite phase. The obtained electron diffraction patterns of these three different phases corroborate this result. According to the EDX analysis, the pseudobrookite phase has a composition of

$$Mg_xFe_{2-2x}Ti_{1+x}O_5 \quad \text{with } 0 \leq x \leq 1$$

It is marked as point P1 in the aforementioned phase diagram. The corresponding spinel phase in equilibrium is marked at P2. The spinel phase observed differs from the latter phase only in respect to its Mg content. Approximately half of the Mg atoms have been replaced by Zn and Ni (24 at.% Zn and 6 at.% Ni, see Table 1). Mg^{2+} can be easily replaced by Ni^{2+} and Zn^{2+}, since the ionic radii of these ions are quite similar (Mg^{2+}: 0·65 Å; Ni^{2+}: 0·72 Å; Zn^{2+}: 0·74 Å).[6] The exchange of Mg^{2+} by Zn^{2+} and other divalent ions is also favoured by their nearly unimpeded diffusion over tetrahedral as well as octahedral lattice sites[7] (Ti^{4+} ions are believed to diffuse only over octahedral sites[8]). These results are in good agreement with those of Hultman *et al.*, who report on Mg_2TiO_4 spinel formation in a TiN–MgO interface.[9]

As expected, the spatial extension of a ferrite–titanate interface mainly depends on the sintering conditions. At 1400 K and 2 h typically interfaces with $d < 3\,\mu m$ are observed. Ceramic layers, prepared by current production techniques like tape-

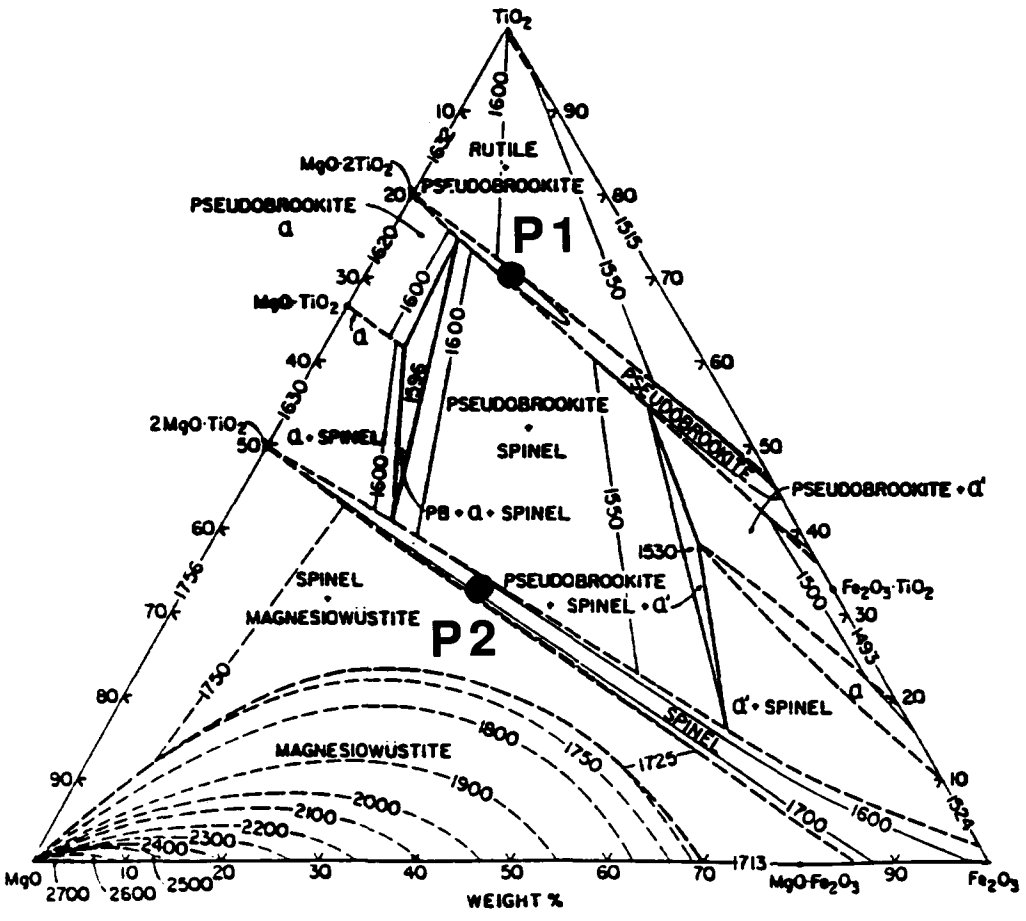

Fig. 7. Phase diagram of the ternary system MgO–TiO_2–Fe_2O_3 according to Ref. 5. The element distribution of the pseudobrookite and spinel phase observed in the $MgTiO_3$–$(Ni,Zn)Fe_2O_4$ interface corresponds to that of P1 and P2 (see also Table 1 and text).

casting or screen-printing, will have thicknesses $>20\,\mu m$. Accordingly, their properties will not be significantly modified by an interface contribution.

In view of the size demands of future integrated passive/active electronic components, however, other preparation methods for electroceramics, especially thin film technologies, are needed. Finally, attention should be drawn to the existence of oxygen disorder and mobility in these oxide materials, which is certainly expected to play an important role in the local and overall electrical properties. Systematic study of such factors would require careful variation in the oxygen potential; it is beyond the scope of the present paper.

In summary, the present SEM and combined TEM/EDX studies have provided information about the spatial extension and the local composition of $(Ni,Zn)Fe_2O_4$–$MgTiO_3$ and $MgTiO_3$–RuO_2 glass interfaces. Both interface properties are essentially controlled by the existing experimental conditions. The sintering time (2 h) at 1400 K was long enough for the interface properties to be essentially representative of local equilibrium. In the case of $(Ni,Zn)Fe_2O_4$–$MgTiO_3$, a $\approx 3\,\mu m$ thick intermediate layer is formed by Fe-rich pseudobrookite and a cation-exchanged spinel phase. In $MgTiO_3$–RuO_2 glass, the formation of $MgSiO_3$ and $PbTiO_3$ is observed at $T > 1100$ K. At lower temperature the interdiffusion of Ti and Mg appears to be the dominant process with no clear sign of phase formation.

Acknowledgements

The authors would like to thank S. Holm (Ferroperm Ltd) for providing the ferrites and H. Salze (Thomson-LCC) for the preparation of the samples. The authors would also like to thank P. Kopold and Prof. M. Rühle (MPI für Metallforschung, Stuttgart, Germany) for their kind help and support of the transmission electron microscope studies. Financial support by the European Community (Contract No. BREU-0051) is gratefully acknowledged.

References

1. LeCorre, A., Kranzmann, A., Nicoloso, N., Brook, R. J., Maier, J. & Maglione, M., Resistor inks: Conductivity, microstructure and interfaces in RuO_2/glass composites. In *Proceedings of the Second Conference of the European Ceramic Society*, Augsburg, FRG, 11–14 September 1991.
2. LeCorre-Frisch, A., Thesis, University of Stuttgart, 1992.
3. Zaluzec, N. J., In *Introduction to Analytical Electron Microscopy*, ed. J. J. Hren, J. I. Goldstein & D. C. Joy. Plenum Press, New York, 1979, p. 121.
4. Bischoff, E., Thesis, University of Stuttgart, 1986.

5. Woermann, E., Brezny, B. & Muan, A., Phase equilibria in the system MgO–iron oxide–TiO_2 in air. *Am. J. Sci.*, **267-A** (1969) 463.
6. Greenwood, N. N., *Ionenkristalle, Gitterdefekte und Nichtstöchiometrische Verbindungen.* Verlag Chemie, Weinheim, Germany, 1973, p. 40.
7. Mozzi, R. L. & Paladino, A. E., Cation distributions in nonstoichiometric magnesium ferrite. *J. Chem. Phys.*, **39** (1963) 435.
8. Tellier, J. C. & Lensen, M., Mg–Fe^{3+} spinels with substitutions. In *Magnetic and other Properties of Oxides and Related Compounds*, Vol. 4, Part B. Landolt-Börnstein, Springer-Verlag, Berlin, Heidelberg, New York, 1970, p. 216.
9. Hultman, L., Hesse, D. & Chiou, W.-A., Mg–Ti-spinel formation at the TiN/MgO interface by solid state reaction: confirmation by high-resolution electron microscopy. *J. Mater. Res.*, **6** (1991) 1744.